Tokyo, Japan). HepG2, PLC/PRF/5, Huh7, HLE and HLF cells were maintained in Dulbecco's modified Eagle's medium containing 10% fetal bovine serum. KIM-1 and KYN2 was maintained in RPMI medium containing 10% fetal bovine serum.

Antibodies and chemicals

The antibodies used included: anti-HSF1, ERK1/2, phosphor-ERK1/2, MAPK kinase (MEK), phospho-MEK, phosphor- efficiently activated epidermal growth factor receptor (EGFR), cyclin D1, cdc2, CDK4, phospho-IκBα, IκB kinase gamma (IKKγ), IKKβ, caspase-3 and Bcl-X_L (Cell Signaling Biotechnology, Danvers, MA); anti-HSP90, HSP72, β-actin and proliferating cell nuclear antigen (PCNA) (Santa Cruz Biotechnology, Santa Cruz, CA); anti-EGFR (Millipore, Billerica, MA); anti-HSP70/HSP72 (Enzo Life science, NY); and anti-BAG3 (Abcam, Cambridge, UK).

Biochemical and immunohistochemical analyses

Protein lysates were prepared from tissues and cultured cells, separated by sodium dodecyl sulfate–polyacrylamide gel electrophoresis, transferred onto Immobilon membranes (Millipore) and analyzed by immunoblotting. Total cellular RNA was extracted using Trizol reagent (Invitrogen, Carlsbad, CA), then cDNA was synthesized using SuperScript II (Invitrogen), and expression of specific messenger RNAs (mRNAs) was quantified using real-time PCR and normalized against glyceraldehyde-3-phosphate dehydrogenase mRNA expression. Details of real-time PCR conditions and primer sequences are available in Supplementary Materials and methods, available at *Carcinogenesis* Online. Immunohistochemical staining was performed on formalin-fixed, paraffin-embedded tissue sections using immunoperoxidase methods, as described previously (15). For array analysis, we used the Human WG-6 BeadChip-kit (Illumina, San Diego, CA) in accordance with the instructions from the manufacturer (details are given in Supplementary Materials and methods, available at *Carcinogenesis* Online).

Establishment of HSF1-knockdown cells

A HSF1 small hairpin RNA (shRNA) plasmid and negative control plasmid were purchased from SABiosciences (QIAGEN, Valencia, CA). The shRNA sequences targeting HSF1 were from position 5′-CAGGTTGTTCATAGTCAGAAT-3′ as in the nucleotide sequence of HSF1. As a negative control, a shRNA was designed with the sequence 5′-GGAATCTCATTCGATGCATAC-3′. Transfection was achieved using Oligofectamine reagent (Invitrogen) according to the instructions from the manufacturer. To establish stable knockdown cell lines, shRNA plasmids were transfected into KYN2 cells and cultured in the presence of puromycin (Sigma–Aldrich, St Louis, MO).

Cell proliferation and bromodeoxyuridine assay

Cell proliferation in response to HSF1 silencing was determined by trypan blue exclusion assay. DNA synthesis was determined by bromodeoxyuridine assay according to the instructions from the manufacturer (Roche Diagnostics, Basel, Switzerland). The result was expressed as a percentage of the maximum absorbance at 450 nm, based on three independent experiments. Cells were counted using a Coulter Counter (Beckman Coulter, Pasadena, CA).

Apoptosis assay

Assessment of apoptosis was performed by measuring the intensity of the sub-G_1 peak. For the sub-G_1 peak, HSF1 control KYN2 cells or HSF1-knockdown (HSF1 KD) KYN2 cells were tumor necrosis factor alpha (TNF-α) treatment for 24 h. Cells were treated with propidium iodide and then the sub-G_1 peak was analyzed with a fluorescence-activated cell sorting (FACS) flow cytometer (FACSCalibur; Becton Dickinson, San Jose, CA). Terminal deoxynucleotidyl transferase-mediated deoxyuridine triphosphate nick-end labeling (TUNEL) assay was performed in accordance with the manufacturer's instructions (ApopTag kit; Intergen, Burlington, MA).

Animals

HSF1-deficient ($HSF^{-/-}$) mice have been described previously (29). C57BL/6 wild-type (WT) mice were purchased from CLEA Japan (Tokyo, Japan) for use in the experiments, with primary hepatocytes isolated using a collagenase perfusion method as described in a previous report (26). For orthotopic implantation, C.B-17/Icr-scid/scidJcl [severe combined immune-deficient mice (SCID)] mice were obtained from CLEA Japan. All mice were maintained in filter-topped cages on autoclaved food and water at the University of Hokkaido and the Institute for Adult Diseases, Asahi Life Foundation, according to National Institutes of Health (NIH) guidelines. All experimental protocols were approved by the ethics committee for animal experimentation at Hokkaido University and Asahi Life Foundation. Orthotopic implantation of KYN2 cells and KYN2 transfectants were performed as described previously (30). Briefly, mice were inoculated orthotopically with 5×10^6 HSF1 control ($n = 12$) and HSF1 KD ($n = 12$) cells in 100 µl of phosphate-buffered saline, injected into the liver. Mice were killed 6 weeks after inoculation and autopsies were performed immediately. In the lipopolysaccharide (LPS)/D-galactosamine (GalN)-induced liver injury model, mice were injected intraperitoneally with LPS (20 lg/kg; Sigma) and GalN (1000 mg/kg; Wako, Osaka, Japan) (24).

Patients and tissue samples

For immunohistochemical analysis, a total of 226 adult patients with HCC who underwent curative resection between 1997 and 2006 at Hokkaido University Hospital were enrolled in this study. A preoperative clinical diagnosis of HCC was required to meet the diagnostic criteria of the American Association for the Study of Liver Diseases. Briefly, inclusion criteria were as follows: (i) distinctive pathological diagnosis, (ii) no preoperative anticancer treatment or distant metastases, (iii) curative liver resection (exclusion of extrahepatic tumor spread/metastasis) and (iv) complete clinicopathological and follow-up data. The study protocols were approved by the institutional review board and performed in compliance with the Helsinki of Declaration. Written informed consent was obtained from as many of the patients who were alive as possible (deceased cases were approved for use without written informed consent). Histological diagnosis was made according to World Health Organization criteria. The main clinicopathological features are presented in Table I. During follow-up, clinical evaluations and biochemical tests were performed every 1–3 months. Patients underwent triphasic computed tomography of the liver every 2–3 months.

Statistical analysis

Data are expressed as mean ± standard error of the mean (SEM). Significant differences were detected using non-parametric testing. Correlations between protein expression and clinicopathological features of the specimens were assessed, and the resulting data were analyzed using the χ^2 test and Fisher's exact test. Cumulative survival rate was calculated from the first date of treatment using the Kaplan–Meier life-table method. Differences were evaluated by log-rank testing. Independent factors for survival were assessed with the Cox proportional hazard regression model. Differences between the two groups were analyzed using the log-rank test. Statistical analyses were performed using Stat View software (version 5.0; SAS Institute, Cary, NC). Values of $P < 0.05$ were considered significant.

Results

Effect of HSF1 on tumor growth

We first investigated expression of HSF1 in cultured HCC cell lines. HSF1 expression was detected in all eight HCC cell lines analyzed. KYN2 cells showed significantly higher expression of HSF1 than other cell lines (Figure 1A). To further elucidate the functional role of HSF1 in HCC, we established HSF1 KD KYN2 cells by expressing the shRNA against HSF1 or control shRNA. To evaluate the effects of HSF1 on cell growth, we measured cell numbers at several time points and found that the growth of HSF1 KD cells was significantly inhibited compared with control cells (HSF1 control) (Figure 1B). Cell cycle regulators including PCNA, cyclin D1, cdc2 and CDK4 were suppressed in HSF1 KD cells compared with HSF1 control cells (Figure 1C). These results indicate that HSF1 enhances HCC cell growth. Concordantly, HSF1 KD reduced DNA synthesis as measured by bromodeoxyuridine incorporation (Figure 1D).

To evaluate the effects of HSF1 on HCC *in vivo*, orthotopic xenografts were established by HSF1 control and HSF1 KD KYN2 cells in nude mice. Maximum primary tumor diameters and tumor volumes were significantly decreased in HSF1 KD xenografts compared with HSF1 control ones (Figure 1E), suggesting that HSF1 accelerated HCC tumor growth *in vivo*. We confirmed that the tumor of HSF1 KD cells showed significantly lower expression of HSF1 and PCNA than the tumor of HSF1 control cells (Figure 1E).

We performed gain-of-function experiments for HSF1 *in vitro*. No apparent changes in cell growth were seen with overexpression of HSF1 in HCC cell lines with low HSF1 expression (Supplementary Figure 1, available at *Carcinogenesis* Online), whereas cell growth was reduced in HSF1 KD experiments, as above. Based on these

Table I. HSF1, BAG3 expression and clinicopathological variables in HCC

Parameter	Total	HSF1		*P*	BAG3		*P*
		High	Low		High	Low	
		n = 115	*n* = 111		*n* = 112	*n* = 114	
		≥30	<30		≥25	<25	
Age (years)							
≥60	126	66	60	0.69	59	67	0.42
<60	100	49	51		53	47	
Sex							
Male	185	95	90	0.86	94	91	0.49
Female	41	20	21		18	23	
Etiology							
HBsAg(+)/HCV(−)	85	45	40	0.70	39	46	0.67
HBsAg(−)/HCV(+)	84	43	41		44	40	
HBsAg(+)/HCV(+)	6	4	2		2	4	
HBsAg(−)/HCV(−)	51	23	28		27	24	
Cirrhosis							
Presence	121	64	57	0.59	62	59	0.59
Absence	105	51	54		50	55	
Tumor size (cm)							
<5	149	67	82	0.017*	66	83	0.035*
≥5	77	48	29		46	31	
No. of tumor nodules							
Solitary	168	78	90	0.032*	79	89	0.22
Multiple (≥2)	58	37	21		33	25	
TNM stage							
I and II	139	62	77	0.017*	63	76	0.11
III and IV	87	53	34		49	38	
BCLC stage							
A	81	27	54	<0.001*	32	49	0.065
B	108	64	44		58	50	
C	37	24	13		22	15	
Differentiation							
Well	36	11	25	0.010*	10	26	0.014*
Moderate	143	74	69		75	68	
Poor	47	30	17		27	20	
Capsular formation							
Presence	184	95	89	0.73	91	93	1.0
Absence	42	20	22		21	21	
Vascular invasion							
Present	37	24	13	0.073	22	15	0.21
Absent	189	91	98		90	99	
Serum AFP level							
<20	117	53	64	0.086	52	65	0.14
≥20	109	62	47		60	49	

AFP, alpha-fetoprotein; BCLC, Barcelona Clinic Liver Cancer; HCV, hepatitis C virus; TNM, tumor node metastasis.
*Significant *P* value.

findings, we concluded that HSF1 expression is a necessary condition for cell growth, but it is not a sufficient condition. We, therefore, did not further investigate gain of function of HSF1.

Impaired EGF-mediated MEK/ERK activation in HSF1 KD cells and HSF1$^{-/-}$ hepatocytes

Activation of the MEK/ERK pathway regulates many important cellular processes in carcinogenesis. To further elucidate the function of HSF1 on tumor growth, we investigated the cascade of MAPK. In WT hepatocytes and HSF1 control cells, EGF, a potent activator of MAPK, efficiently activated EGFR, MEK1/2 and ERK1/2 (Figure 2A). In contrast, activation of EGFR, MEK1/2 or ERK1/2 was significantly decreased in HSF-knockout mice (HSF$^{-/-}$) hepatocytes and HSF1 KD cells (Figure 2A and B). Regarding protein levels of EGFR, MEK1/2 and ERK1/2, EGFR protein levels were significantly decreased in HSF1$^{-/-}$ hepatocytes and HSF1 KD compared with controls, whereas other proteins were unchanged (Figure 2A and B). This result was consistent with the previous report (31). Immunohistochemical staining revealed that HSF1 control tumor showed strong phosphorylated ERK1/2 levels, whereas almost no ERK1/2 activation was observed in HSF1 KD tumors (Figure 2C).

Role of HSF1 in TNF-α-induced apoptosis

Since tumor growth inhibition is caused mainly by increased cell death and decreased cellular proliferation, we compared numbers of apoptotic cell deaths in HSF1 control and HSF KD xenografts using the TUNEL assay. Significantly more apoptotic tumor cells were found in HSF1 KD tumors than in HSF1 control tumors (Figure 3A). Next, we examined whether HSF1 was involved in apoptosis *in vitro*. FACS analysis showed very few apoptotic cells in HSF KD or HSF control in the absence of any stimuli. In contrast, treatment with TNF-α, a potent inducer of apoptosis, caused more extensive apoptotic cell death in HSF1 KD cells (23.9%) than in HSF control cells (8.7%) (Figure 3B). Furthermore, we also confirmed increased TNF-α-induced apoptosis in HSF KD cells as determined by TUNEL assay and caspase-3 activation (Figure 3C and D). To examine whether HSF1 is required for TNF-α-induced liver apoptosis *in vivo*, we used an LPS/GalN liver injury model that depends on TNF-α-mediated apoptosis (32). At 7 h LPS/GalN

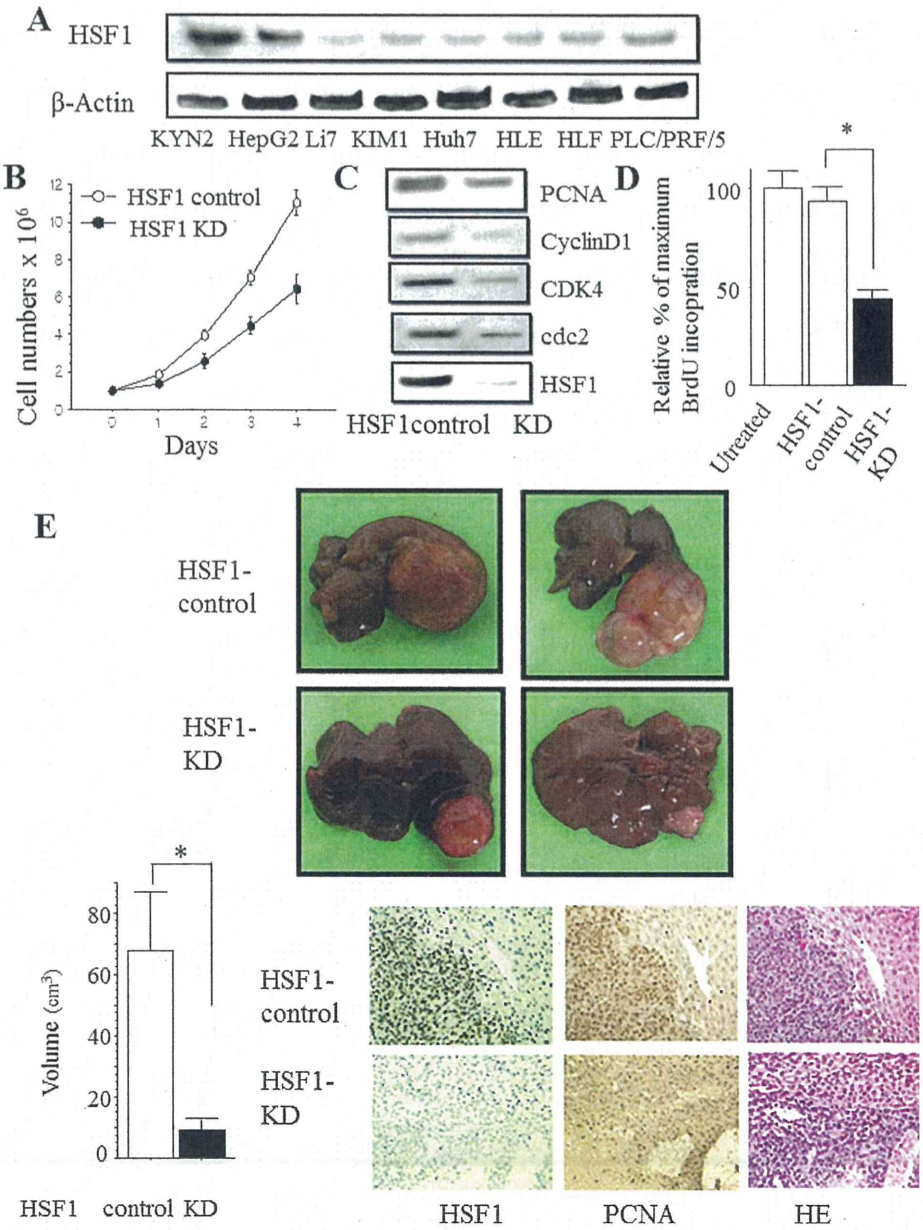

Fig. 1. Role of HSF1 in HCC growth. (**A**) Expression of HSF1 in the eight indicated HCC cell lines was determined by western blot analysis, using β-actin as a control. (**B**) Cell growth of HSF1 control KYN2 cells and HSF1 KD KYN2 cells was measured by counting the number of cells. One representative experiment from three experiments is shown. Data are plotted as mean ± SEM. (**C**) Expression of cell-cycle-related protein in HSF1 control KYN2 cells and HSF1 KD KYN2 cells, as determined by western blot analysis. (**D**) Cells were pulsed with BrdU (10 mmol/l) for 4 h. Optical density values are expressed as a percentage relative to the group expressing control. $^*P < 0.05$. Bars: SEM. (**E**) Growth appearance of HSF1 KD and HSF1 control cells in SCID mice after orthotopic implantation (upper panel). Orthotopic tumor volume was measured. Data are expressed as mean ± SEM (HSF1 control, $n = 12$; HSF1 KD, $n = 12$). $^*P < 0.05$. Bars: SEM (lower left panel). HE and immunohistochemical staining for HSF1 and PCNA (original magnification: ×40): lower right panel. BrdU, bromodeoxyuridine; HE, hematoxylin and eosin.

administration, $HSF^{-/-}$ exhibited marked alanine aminotransferase elevation (Figure 3E), severe histological liver damage and hepatocyte apoptosis compared with WT mice (Figure 3E). This was also in accordance with the notable depression of HSF1 inducing apoptosis *in vitro*.

HSF1 is involved in TNF-α-mediated NF-κB activation

Regarding the association between HSF1 and antiapoptosis, expression of bcl-2-associated athanogene domain 3 (BAG3) was reportedly reduced in HSF1 KD cells compared with control cells (7,11). In addition, microarray array analysis showed that BAG3 was dramatically downregulated in HSF1 KD cells compared with HSF1 control cells (Supplementary Table I, available at *Carcinogenesis* Online). Immunoblot analysis showed that BAG3 protein expression was reduced in $HSF1^{-/-}$ hepatocytes and HSF1 KD cells relative to the respective controls (Figure 4A and B). Meanwhile, activation of IKK and NF-κB pathway represents one of the most important antiapoptotic signals. In addition, BAG3 is also reported to control proteasomal degradation of IKKγ, the regulatory subunit (also called NF-κB essential modulator) of the IKK complex, and

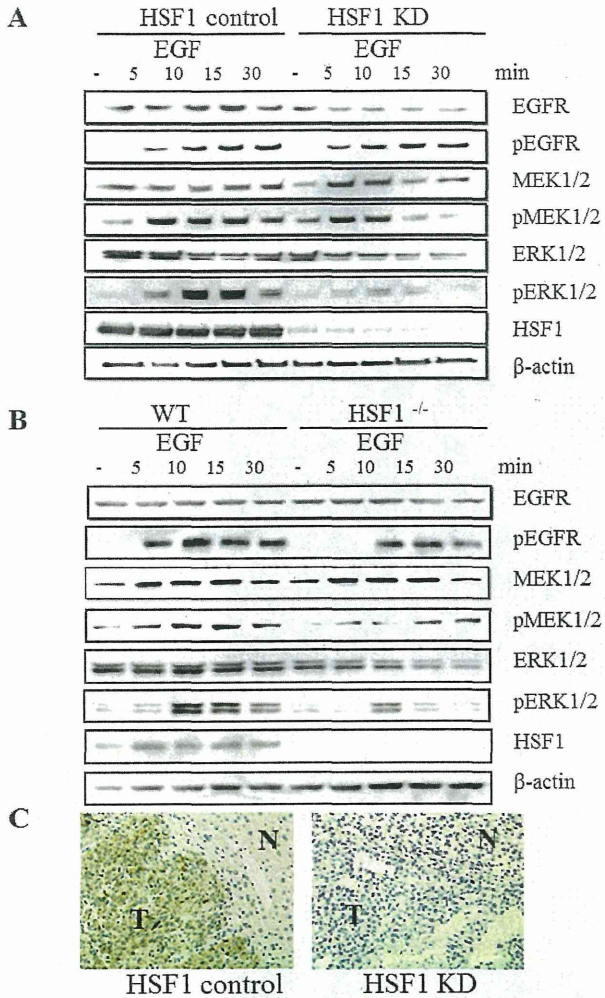

Fig. 2. EGF-mediated MEK/ERK activation is impaired in HSF1 KD cells and HSF1$^{-/-}$ hepatocytes. (**A**) HSF1 control and KD cells were treated with EGF (10 ng/ml), lysed at the indicated times, gel separated and immunoblotted with antibodies against indicated proteins. (**B**) HSF1 WT and HSF$^{-/-}$ hepatocytes were treated with TNF-α (30 ng/ml), lysed in indicated times, gel separated and immunoblotted with antibodies against indicated proteins. (**C**) Representative phosphorylated ERK (p-ERK) staining of orthotopic tumors of HSF1 control and KD cells (original magnification: ×40). N, non-cancerous liver; T, tumor.

NF-κB activity (33). Regarding the NF-κB pathway, NF-κB activation by TNF-α was decreased in HSF1 KD cells compared with the control cells (Figure 4A). In contrast, without any treatment, basal NF-κB activity was very weak and no differences were apparent between HSF1 control cells and HSF1 KD cells (Figure 4A). Consistent with this, microarray analysis showed no apparent differences in the expression of typical NF-κB-regulated genes. We also performed NF-κB pathway analysis and found that the pathway was not overrepresented by the microarray results (Supplementary Figure 2, available at *Carcinogenesis* Online). Next, we investigated whether HSF1 is involved in TNF-α-mediated NF-κB activation and found that phosphorylated Iκk-B (p-IκB), a marker of NF-κB activation, was significantly decreased in HSF$^{-/-}$ hepatocytes and HSF1 KD cells compared with their controls. As expected, IKKγ protein levels were dramatically reduced in HSF1$^{-/-}$ hepatocytes and HSF1 KD cells compared with their controls (Figure 4A and B). To investigate whether decreased IKKγ protein was degraded via proteasome, we used the proteasomal inhibitor, MG-132, and found that protein levels of IKKγ in HSF1 KD cells recovered with the inhibitor, whereas protein expression of BAG3 was unchanged (Figure 4C). Although mRNA levels of BAG3 were significantly downregulated in HSF1 KD cells compared with HSF1 control cells, mRNA levels of IKKγ were not changed (Figure 4D). HSP70 mRNA and protein levels were similar between HSF1 control and HSF1 KD cells (Figure 4A–D). These results suggest that HSF1 positively regulated BAG3 expression, which stabilized the IKKγ protein necessary for NF-κB activation. Immunohistochemical staining revealed that downregulation of HSF1 dramatically reduced BAG3 levels in HSF1 KD xenografts compared with the HSF1 control xenografts.

We performed real-time PCR analysis of the putative NF-κB-regulated antiapoptotic genes. The levels of A20, cellular inhibitor of apoptosis 2 (c-IAP2) RNA expression were decreased in HSF1 KD cells by TNF-α-mediated compared with HSF1 control cells, whereas cylindromatosis, cIAP1 were unchanged (Figure 4E). These results suggest that HSF1 plays an important role in tumor growth via MAPK-mediated cellular proliferation and NF-κB-mediated antiapoptosis.

HSF1 and BAG3 were frequently overexpressed in human HCCs

To analyze the involvement of HSF1 in HCCs, we examined expression levels of HSF1 in human primary HCCs. Immunoblot analysis showed that levels of HSF1 in HCC tissues were significantly higher than in non-cancerous liver tissues in 5 of 10 samples (50%) (Figure 5A). We tested 226 samples from tumor tissues of patients with HCCs by immunohistochemistry. The median percentage of positive cells was 30% (range: 0–90.0%) and we divided patients into two groups of high expressers and low expressers based on the percentage of HSF1-positive cells using a cutoff level of 30%, representing the median value of HSF1. We found that 50.9% (115/226) of tumor samples showed high HSF1 expression. Typical examples of high HSF1 expression samples are shown in Figure 5B. The characteristics of patients in this analysis are shown in Table I. Significant differences were apparent between high and low HSF1 expression groups in terms of tumor size ($P = 0.017$), tumor node metastasis stage ($P = 0.017$), Barcelona Clinic Liver Cancer stage ($P < 0.001$), number of tumor nodules ($P = 0.032$) and histological grade ($P = 0.010$) (Table I), but no significant correlations were observed between HSF1 expression and other clinicopathological variables such as etiology or cirrhosis (Table I). Furthermore, patients with tumors showing HSF1 overexpression displayed significantly shorter overall survival (median: 75.2 months) compared with patients whose tumors showed HSF1 low expression (median: 136.0 months; $P = 0.004$, log-rank test) (Figure 5C). These findings suggest that overexpression of HSF1 was frequently observed in human HCCs, particularly in tumors exhibiting aggressive features.

To explore the pathological relationship between HSF1 and BAG3 in HCC samples, we performed immunohistochemical analysis for BAG3 in 226 HCC samples, which were also analyzed for HSF1 immunohistochemistry. The median percentage of positive cells was 25% (range: 0–85.0%) and we divided them into two groups—high expressers and low expressers—based on the percentage of BAG3-positive cells using a cutoff level of 25%, representing the median value of BAG3. Representative examples of immunohistochemical reactivity for BAG3 are shown in Figure 5B. Expressions of BAG3 protein were significantly increased in HCC specimens, whereas no or only low BAG3 expression was seen in adjacent non-cancerous tissue. BAG3 expression correlated significantly with histological grade ($P = 0.014$), and tumor size ($P = 0.035$), but no significant correlations were observed between BAG3 expression and other clinicopathological variables (Table I). Furthermore, a positive correlation between expressions of HSF1 and BAG3 was found in HCC ($P < 0.05$; Figure 5D) and patients with tumors showing BAG3 overexpression displayed significantly shorter overall survival (median: 84.0 months) compared with those patients whose tumors showed BAG3 low expression (median: 134.2 months; $P = 0.015$, log-rank test) (Figure 5E). Multivariate Cox regression

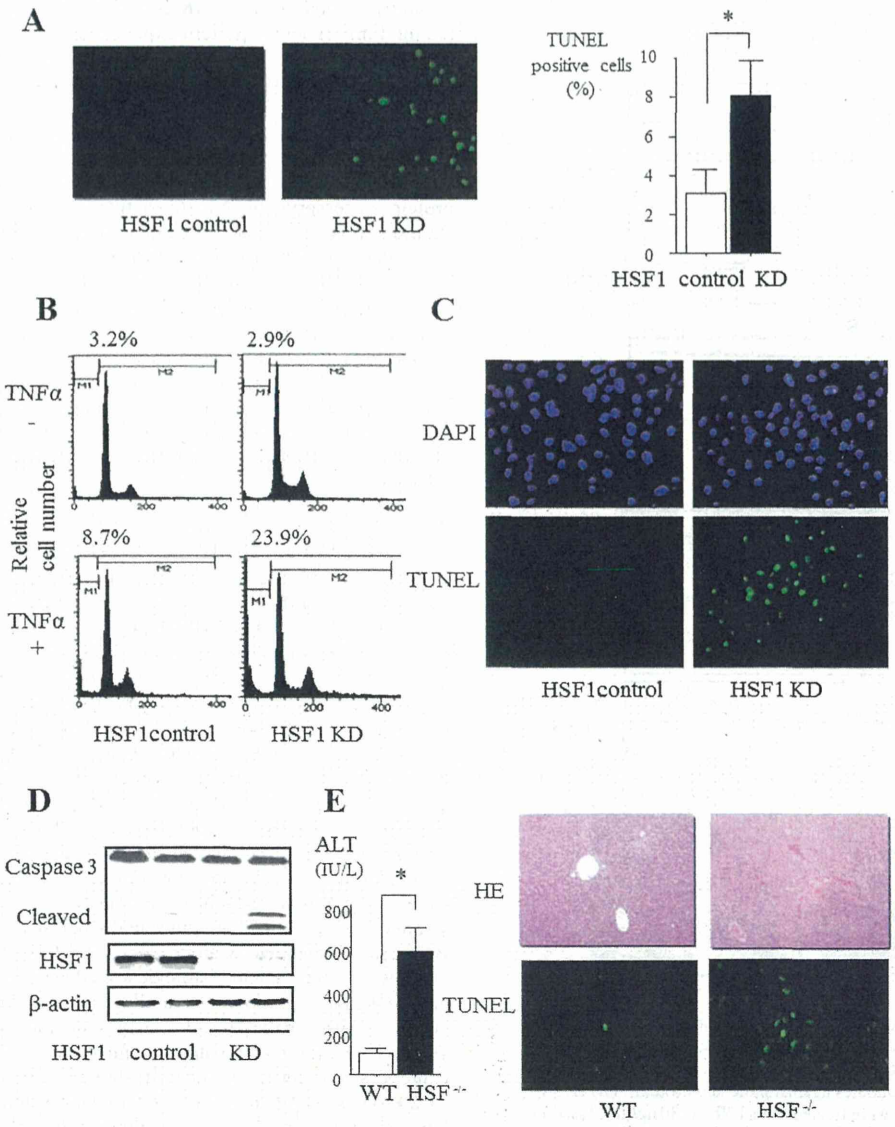

Fig. 3. Antiapoptotic effect of HSF1 in HCC cells and hepatocytes. (**A**) TUNEL staining was performed in tumors of HSF1 control and HSF1 KD cells from orthotopic implanted mice (left panel). TUNEL-positive cells were counted in tumors of HSF1 control and HSF1 KD cells. $^*P < 0.05$. Bars: SEM (right panel). (**B**) Apoptotic cells were evaluated by FACS at 24 h after incubation with TNF-α (30 ng/ml). Values indicate percentages of cells with sub-G_1 DNA content. Representative data are shown from three independent experiments. (**C**) TUNEL staining was performed in HSF1 control and KD cells after incubation with TNF-α. (**D**) Protein expressions of caspase 3, HSF1 and β-actin in TNF-α-treated HSF1 control and KD cells were determined by western blot analysis. (**E**) Serum ALT levels 7 h after injection of WT and HSF1$^{-/-}$ mice with LPS (5 μg/kg) and GalN (500 mg/kg). $^*P < 0.05$, compared with WT mice (left panel). HE and TUNEL stainings were performed in sections of livers obtained 7 h after injecting LPS (5 μg/kg) and GalN (500 mg/kg) into WT and HSF1$^{-/-}$ mice (right panel). ALT, alanine aminotransferase; DAPI, 4′,6-diamidino-2-phenylindole; HE, hematoxylin and eosin.

analysis identified high HSF1 expression (hazard ratio: 2.07; $P = 0.04$) as an independent prognostic factor for overall survival (Table II).

Discussion

As a master regulator of the heat shock response, HSF1 enhances organism survival and longevity in the face of environmental challenges. However, HSF1 can also act to the detriment of organisms by supporting malignant transformation (34). As reported previously, loss of HSF1 negatively impacts tumorigenesis driven by p53 or Ras mutations (8,16). Since HSF1 does not act as a classic oncogene, the increased resistance to proteotoxic stress induced by HSF1 was suggested to support tumor initiation and growth by enabling cells to accommodate the genetic alterations that accumulate during malignancy (35). However, the specific mechanisms by which HSF1 may support the growth of tumors are not well understood. Here, we have demonstrated that HSF1 has detrimental effects on liver tumor growth. We also proposed that the antiapoptotic effect of HSF1 may play a role in HCC tumor growth.

To clarify the mechanisms underlying this effect, we investigated associations between HSF1 and the NF-κB signaling pathway. Although, in a previous study, heat shock blocked the degradation of IκB (36) and nuclear translocation of NF-κB, the recent literature has reported that the presence of constitutively active HSF1 does not block TNF-α-induced activation of the NF-κB pathway or expression of a set of NF-κB-dependent genes (37). The current study established HSF1 KD cells and showed that HSF1 was necessary for TNF-α-induced NF-κB activation. We analyzed the function of BAG3 as a candidate for the molecule connecting HSF1 with NF-κB activation. BAG3 has reportedly been characterized by the

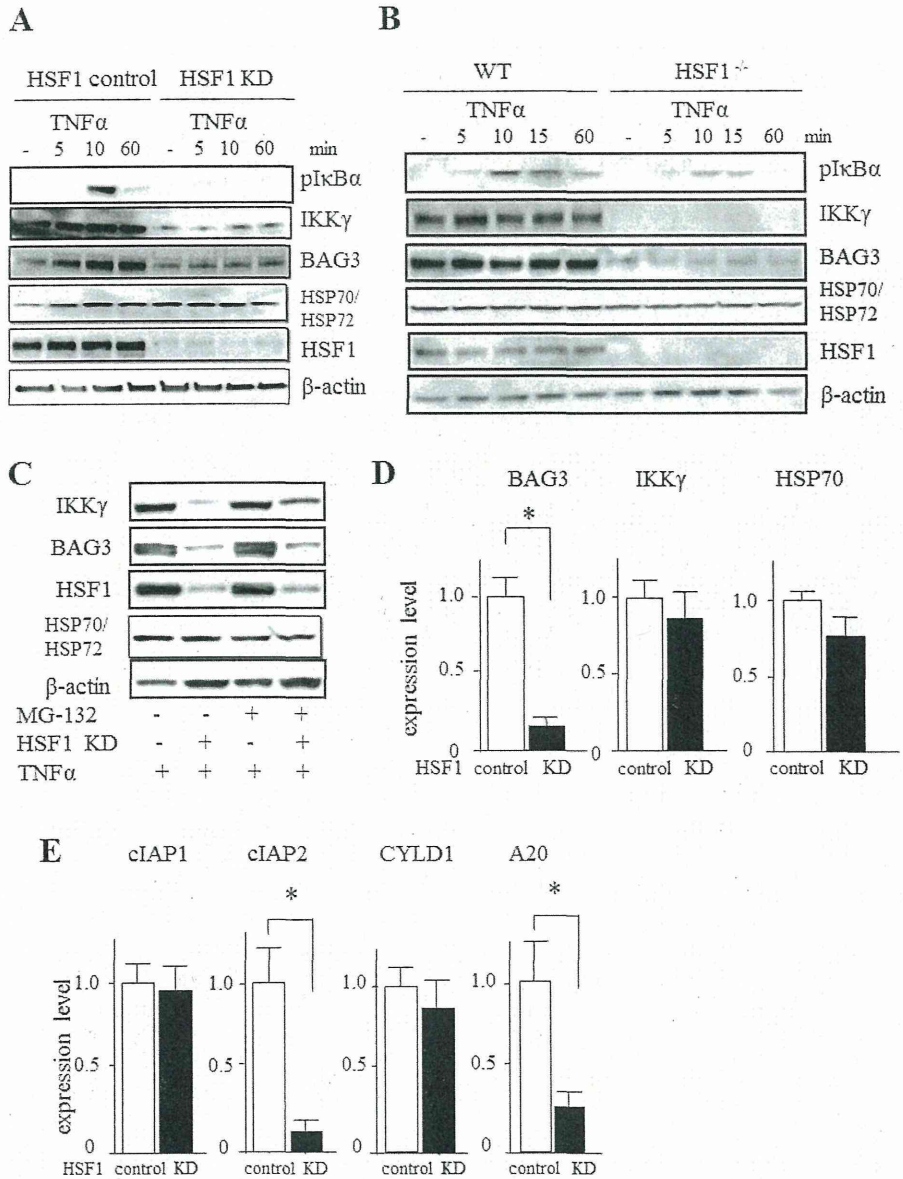

Fig. 4. HSF1 is involved in TNF-α-mediated NF-κB activation. (**A**) HSF1 control and KD cells were treated with TNF-α (30 ng/ml), lysed at the indicated times, gel separated and immunoblotted with antibodies against the indicated proteins. (**B**) HSF1 WT and HSF$^{-/-}$ hepatocytes treated with TNF-α (30 ng/ml), lysed at the indicated times, gel separated and immunoblotted with antibodies against the indicated proteins. (**C**) HSF1 control and KD cells were treated with TNF-α (30 ng/ml) with or without MG-132, lysed at 24 h, gel separated and immunoblotted with antibodies against indicated proteins. (**D**) Relative mRNA levels for BAG3, IKKγ and HSP70 in HSF1 control and KD cells determined by real-time PCR. Data are expressed as mean ± SEM ($n = 4$ per group). *$P < 0.05$. Bars: SEM. (**E**) Relative mRNA levels for antiapoptosis-related gene in HSF1 control and KD cells as determined by real-time PCR. Data are expressed as mean ± SEM ($n = 4$ per group). *$P < 0.05$. Bars: SEM. CYLD, cylindromatosis.

interaction with a variety of partners (Raf-1, steroid hormone receptors and HSP70) and is involved in regulating a number of cellular processes, particularly those associated with antiapoptosis (38). This molecule was expressed in response to stressful stimuli in a number of normal cell types and appears constitutively in a variety of tumors (33,39), and gene expression is regulated by HSF1 (40). In addition, knockdown of BAG3 protein decreased IKKγ levels, increasing tumor cell apoptosis and inhibiting tumor growth (33). Based on these considerations, we investigated whether attenuating HSF1 would enhance IKKγ protein expression, and data with MG-132 show that proteasomal degradation of IKKγ is enhanced in HSF1 KD cells. In addition, knowledge of the role BAG3 plays in preventing the proteasomal turnover of certain proteins suggests that the loss of BAG3 in HSF1 KD cells may be responsible for the enhanced turnover of IKKγ in this setting.

NF-κB activation is a master regulatory step in antiapoptosis. Several mechanisms have been reported regarding this antiapoptotic effect of NF-κB activation (41). NF-κB exerts its prosurvival activity primarily through the induction of target genes, the products of which inhibit components of the apoptotic machinery. These include Bcl-X_L and c-IAP (41), which binds directly to and inhibits the effect of caspases. This study showed that inactivation of NF-κB promoted apoptotic effects against TNF-α in HSF1$^{-/-}$ hepatocytes and HSF1 KD HCC cells. Real-time PCR analyses indicated that expression levels of apoptosis-related genes such as A20 and c-IAP2 were decreased by inhibition of NF-κB activation, whereas apoptosis-related genes such

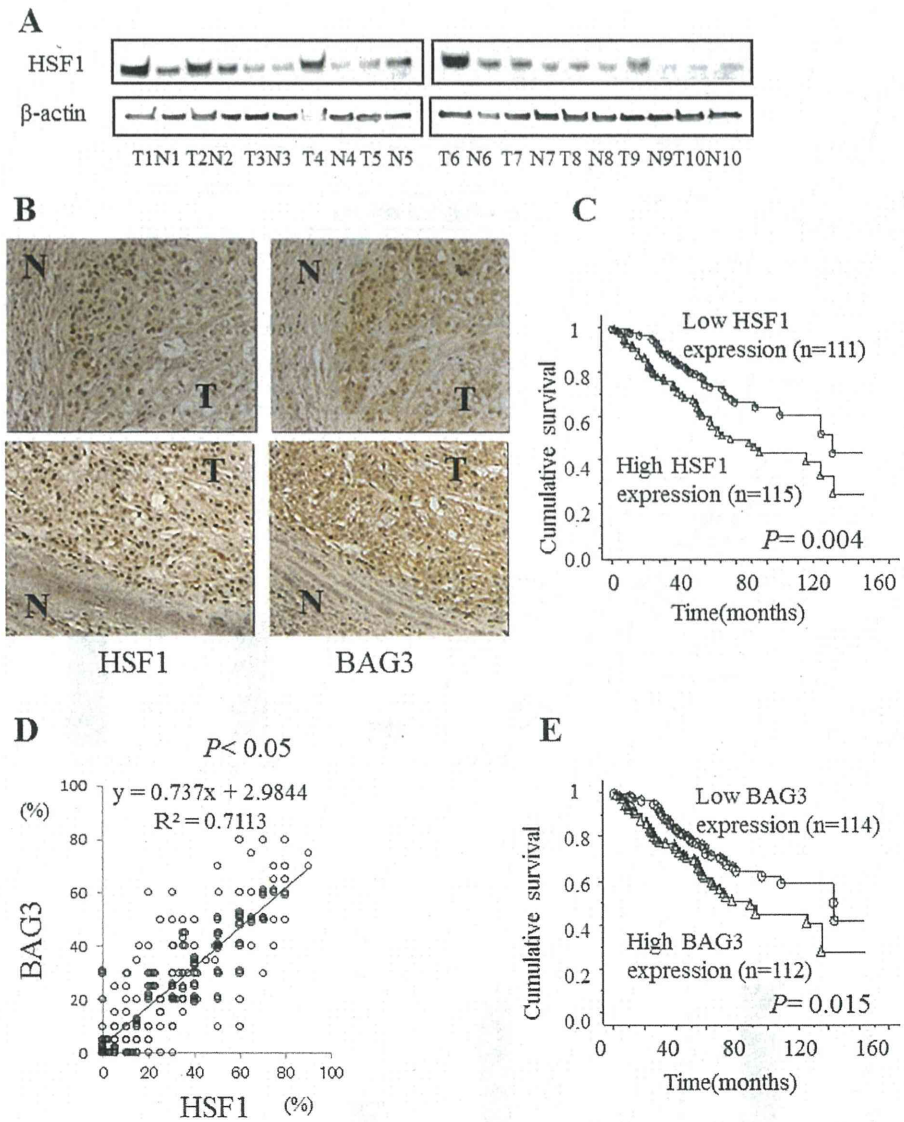

Fig. 5. Overexpression of HSF1 protein in human HCCs and pathological relationship between HSF1 and BAG3 in HCC samples. (**A**) HSF1 protein expression was determined in paired samples of human non-neoplastic liver and HCC by western blot, using β-actin as a control. N, non-cancerous liver; T, tumor. (**B**) Representative HSF1 and BAG3 staining of HCC and surrounding tissue. (**C**) Correlation of HSF1 overexpression with overall survival rates of patients. (**D**) Relationship between BAG3 and HSF1 expression in HCC. Scatterplot of BAG3 versus HSF1 with regression line displaying a correlation according to Spearman's correlation coefficient ($P < 0.01$). (**E**) Correlation of BAG3 overexpression with overall survival rates of patients.

as cIAP1 and cylindromatosis, which are known to be regulated by NF-κB activation, were apparently unaffected. Whether gene expression regulated by NF-κB activity differs between inducible and basal activation remains to be determined.

Regarding the relationship between HSF1 and HCC development, HSF1-deficient mice recently revealed dramatically reduced numbers and sizes of tumors compared with WT controls when tumors were induced by the chemical carcinogen, diethylnitrosamine. The same study suggested that the presence of extensive pathology associated with severe steatosis by diethylnitrosamine was prevented by HSF1 deletion and may be associated with reduced HCC development (42). On the other hand, ablation of IKKγ in liver parenchymal cells caused spontaneous development of HCC in mice, with tumor development preceded by steatohepatitis (43). Based on these observations, we assume that reductions in diethylnitrosamine-induced HCC development among HSF1-deficient mice may be associated with reduced expression of IKKγ, the reduction of which caused the steatosis.

BAG3 is a critical regulator of apoptosis in HSF1-deficient hepatocytes and HSF1 KD HCC cells. Moreover, the relationship between HSF1 and BAG3 has been shown not only in cell cultures and mouse models, but also in human HCC tissue samples; a correlation between HSF1 expression and BAG3 expression was found in HCC. Clinicopathological features and biological results provide a mechanistic link between HSF1 and HCC development via BAG3.

As for the ERK signal, a previous study demonstrated that impairment of JNK and ERK signaling in $HSF1^{-/-}$ MEF cells was caused in part by the reduced expression of EGFR (33). We showed a slight decrease in expression of EGFR among HSF1-deficient hepatocytes and HSF1 KD cells. On the other hand, the level of reduced activation of ERK, as a downstream molecule of EGFR, was larger than expected. However, the detailed mechanisms by which HSF1 regulates MAPK need further investigation.

In conclusion, we found that HSF1 deficiency significantly diminished NF-κB and MAPK activation in HCC hepatocytes and

Table II. Multivariate analysis with a Cox proportional hazards regression model

Characteristic	Univariate analysis	Multivariate analysis	Hazard ratio (95% CI)
Age (≥60 years)	0.22	0.15	
Gender (male)	0.92	0.53	
HCV status (positive)	0.28	0.82	
Cirrhosis (positive)	0.15	0.066	
Tumor size (≥50 mm)	<0.01*	0.011*	2.21 (1.18–4.12)
No. of tumor nodule (multiple)	<0.01*	<0.01*	2.67 (1.38–5.62)
Tumor differentiation (poor)	<0.01*	0.031*	2.34 (1.33–4.11)
Capsular formation (absence)	0.18	0.36	
Vascular invasion (presence)	0.062	0.10	
TNM stage (III + IV versus I + II)	<0.01*	0.020*	2.35 (1.14–4.82)
AFP (≥20 ng/ml)	0.18	0.36	
HSF1 expression (high)	0.018*	0.040*	2.07 (1.22–3.50)
BAG3 expression (high)	0.043*	0.056	

AFP, alpha-fetoprotein; CI, confidence interval; HCV, hepatitis C virus; TNM, tumor node metastasis.
*Significant *P* value.

HCC cells; accordingly, HSF1 deficiency inhibited the development of HCC. Furthermore, clinicopathological analysis demonstrated a significant correlation between HSF1 or BAG3 protein levels and prognosis. Our results demonstrate the importance of HSF1 in human HCCs and suggest inhibition of HSF1 as a novel strategy to target that subset of HCC patients in whom this protein is overexpressed.

Supplementary material

Supplementary Materials and methods, Table I and Figures 1 and 2 can be found at http://carcin.oxfordjournals.org/

Funding

Ministry of Education, Culture, Sports, Science and Technology, Japan (to N.S.); Japan Society for the Promotion of Science (24390185, 24659359); Ministry of Health, Labour and Welfare Japan; Japan Health Sciences Foundation; grants-in-aid for scientific research (22300317) and Uehara Memorial Foundation (to S.M.).

Conflict of Interest Statement: None declared.

References

1. El-Serag,H.B. (2012) Epidemiology of viral hepatitis and hepatocellular carcinoma. *Gastroenterology*, **142**, 1264–1273.e1.
2. Cheng,A.L. *et al.* (2009) Efficacy and safety of sorafenib in patients in the Asia-Pacific region with advanced hepatocellular carcinoma: a phase III randomised, double-blind, placebo-controlled trial. *Lancet Oncol.*, **10**, 25–34.
3. Breuhahn,K. *et al.* (2011) Strategies for hepatocellular carcinoma therapy and diagnostics: lessons learned from high throughput and profiling approaches. *Hepatology*, **53**, 2112–2121.
4. Pirkkala,L. *et al.* (2001) Roles of the heat shock transcription factors in regulation of the heat shock response and beyond. *FASEB J.*, **15**, 1118–1131.
5. Sorger,P.K. (1991) Heat shock factor and the heat shock response. *Cell*, **65**, 363–366.
6. Guertin,M.J. *et al.* (2010) Chromatin landscape dictates HSF binding to target DNA elements. *PLoS Genet.*, **6**, e1001114.
7. Mendillo,M.L. *et al.* (2012) HSF1 drives a transcriptional program distinct from heat shock to support highly malignant human cancers. *Cell*, **150**, 549–562.
8. Page,T.J. *et al.* (2006) Genome-wide analysis of human HSF1 signaling reveals a transcriptional program linked to cellular adaptation and survival. *Mol. Biosyst.*, **2**, 627–639.
9. Dai,C. *et al.* (2007) Heat shock factor 1 is a powerful multifaceted modifier of carcinogenesis. *Cell*, **130**, 1005–1018.
10. Hayashida,N. *et al.* (2006) A novel HSF1-mediated death pathway that is suppressed by heat shock proteins. *EMBO J.*, **25**, 4773–4783.
11. Jacobs,A.T. *et al.* (2007) Heat shock factor 1 attenuates 4-hydroxynonenal-mediated apoptosis: critical role for heat shock protein 70 induction and stabilization of Bcl-XL. *J. Biol. Chem.*, **282**, 33412–33420.
12. Vydra,N. *et al.* (2006) Spermatocyte-specific expression of constitutively active heat shock factor 1 induces HSP70i-resistant apoptosis in male germ cells. *Cell Death Differ.*, **13**, 212–222.
13. Neckers,L. *et al.* (2012) Hsp90 molecular chaperone inhibitors: are we there yet? *Clin. Cancer Res.*, **18**, 64–76.
14. Khalil,A.A. *et al.* (2011) Heat shock proteins in oncology: diagnostic biomarkers or therapeutic targets? *Biochim. Biophys. Acta*, **1816**, 89–104.
15. Chuma,M. *et al.* (2003) Expression profiling in multistage hepatocarcinogenesis: identification of HSP70 as a molecular marker of early hepatocellular carcinoma. *Hepatology*, **37**, 198–207.
16. Cai,L. *et al.* (2003) The tumor-selective over-expression of the human Hsp70 gene is attributed to the aberrant controls at both initiation and elongation levels of transcription. *Cell Res.*, **13**, 93–109.
17. Min,J.N. *et al.* (2007) Selective suppression of lymphomas by functional loss of Hsf1 in a p53-deficient mouse model for spontaneous tumors. *Oncogene*, **26**, 5086–5097.
18. Santagata,S. *et al.* (2011) High levels of nuclear heat-shock factor 1 (HSF1) are associated with poor prognosis in breast cancer. *Proc. Natl Acad. Sci. USA*, **108**, 18378–18383.
19. Dudeja,V. *et al.* (2011) Prosurvival role of heat shock factor 1 in the pathogenesis of pancreatobiliary tumors. *Am. J. Physiol. Gastrointest. Liver Physiol.*, **300**, G948–G955.
20. Hoang,A.T. *et al.* (2000) A novel association between the human heat shock transcription factor 1 (HSF1) and prostate adenocarcinoma. *Am. J. Pathol.*, **156**, 857–864.
21. Ishiwata,J. *et al.* (2012) State of heat shock factor 1 expression as a putative diagnostic marker for oral squamous cell carcinoma. *Int. J. Oncol.*, **40**, 47–52.
22. Kojiro,M. *et al.* (2009) Pathologic diagnosis of early hepatocellular carcinoma: a report of the international consensus group for hepatocellular neoplasia. *Hepatology*, **49**, 658–664.
23. Fabregat,I. *et al.* (2007) Survival and apoptosis: a dysregulated balance in liver cancer. *Liver Int.*, **27**, 155–162.
24. Nakagawa,H. *et al.* (2011) Apoptosis signal-regulating kinase 1 inhibits hepatocarcinogenesis by controlling the tumor-suppressing function of stress-activated mitogen-activated protein kinase. *Hepatology*, **54**, 185–195.
25. Sun,B. *et al.* (2008) NF-kappaB signaling, liver disease and hepatoprotective agents. *Oncogene*, **27**, 6228–6244.
26. Maeda,S. *et al.* (2005) IKKbeta couples hepatocyte death to cytokine-driven compensatory proliferation that promotes chemical hepatocarcinogenesis. *Cell*, **121**, 977–990.
27. Beeram,M. *et al.* (2005) Raf: a strategic target for therapeutic development against cancer. *J. Clin. Oncol.*, **23**, 6771–6790.
28. Whittaker,S. *et al.* (2010) The role of signaling pathways in the development and treatment of hepatocellular carcinoma. *Oncogene*, **29**, 4989–5005.
29. Inouye,S. *et al.* (2003) Activation of heat shock genes is not necessary for protection by heat shock transcription factor 1 against cell death due to a single exposure to high temperatures. *Mol. Cell. Biol.*, **23**, 5882–5895.
30. Chuma,M. *et al.* (2004) Overexpression of cortactin is involved in motility and metastasis of hepatocellular carcinoma. *J. Hepatol.*, **41**, 629–636.
31. O'Callaghan-Sunol,C. *et al.* (2006) Heat shock transcription factor (HSF1) plays a critical role in cell migration via maintaining MAP kinase signaling. *Cell Cycle*, **5**, 1431–1437.

32. Nowak,M. *et al.* (2000) LPS-induced liver injury in D-galactosamine-sensitized mice requires secreted TNF-alpha and the TNF-p55 receptor. *Am. J. Physiol. Regul. Integr. Comp. Physiol.*, **278**, R1202–R1209.
33. Ammirante,M. *et al.* (2010) IKK{gamma} protein is a target of BAG3 regulatory activity in human tumor growth. *Proc. Natl Acad. Sci. USA*, **107**, 7497–7502.
34. Meng,L. *et al.* (2010) Heat-shock transcription factor HSF1 has a critical role in human epidermal growth factor receptor-2-induced cellular transformation and tumorigenesis. *Oncogene*, **29**, 5204–5213.
35. Solimini,N.L. *et al.* (2007) Non-oncogene addiction and the stress phenotype of cancer cells. *Cell*, **130**, 986–988.
36. Malhotra,V. *et al.* (2002) Heat shock inhibits activation of NF-kappaB in the absence of heat shock factor-1. *Biochem. Biophys. Res. Commun.*, **291**, 453–457.
37. Janus,P. *et al.* (2011) NF-κB signaling pathway is inhibited by heat shock independently of active transcription factor HSF1 and increased levels of inducible heat shock proteins. *Genes Cells*, **16**, 1168–1175.
38. Rosati,A. *et al.* (2011) BAG3: a multifaceted protein that regulates major cell pathways. *Cell Death Dis.*, **2**, e141.
39. Homma,S. *et al.* (2006) BAG3 deficiency results in fulminant myopathy and early lethality. *Am. J. Pathol.*, **169**, 761–773.
40. Franceschelli,S. *et al.* (2008) Bag3 gene expression is regulated by heat shock factor 1. *J. Cell. Physiol.*, **215**, 575–577.
41. Luo,J.L. *et al.* (2005) IKK/NF-kappaB signaling: balancing life and death–a new approach to cancer therapy. *J. Clin. Invest.*, **115**, 2625–2632.
42. Jin,X. *et al.* (2011) Heat shock transcription factor 1 is a key determinant of HCC development by regulating hepatic steatosis and metabolic syndrome. *Cell Metab.*, **14**, 91–103.
43. Luedde,T. *et al.* (2007) Deletion of NEMO/IKKgamma in liver parenchymal cells causes steatohepatitis and hepatocellular carcinoma. *Cancer Cell*, **11**, 119–132.

Received December 4, 2012; revised August 22, 2013; accepted August 28, 2013

Oncogene (2014), 1–13

www.nature.com/onc

ORIGINAL ARTICLE

Cellular senescence checkpoint function determines differential Notch1-dependent oncogenic and tumor-suppressor activities

S Kagawa[1,2,16], M Natsuizaka[1,2,3,16], KA Whelan[1,2], N Facompre[4,5], S Naganuma[1,2,6], S Ohashi[1,2,7], H Kinugasa[1,2,8], AM Egloff[9], D Basu[4,5], PA Gimotty[2,10], AJ Klein-Szanto[11], AJ Bass[12,13], K-K Wong[12,13], JA Diehl[2,14], AK Rustgi[1,2,15] and H Nakagawa[1,2]

Notch activity regulates tumor biology in a context-dependent and complex manner. Notch may act as an oncogene or a tumor-suppressor gene even within the same tumor type. Recently, Notch signaling has been implicated in cellular senescence. Yet, it remains unclear as to how cellular senescence checkpoint functions may interact with Notch-mediated oncogenic and tumor-suppressor activities. Herein, we used genetically engineered human esophageal keratinocytes and esophageal squamous cell carcinoma cells to delineate the functional consequences of Notch activation and inhibition along with pharmacological intervention and RNA interference experiments. When expressed in a tetracycline-inducible manner, the ectopically expressed activated form of Notch1 (ICN1) displayed oncogene-like characteristics inducing cellular senescence corroborated by the induction of G0/G1 cell-cycle arrest, Rb dephosphorylation, flat and enlarged cell morphology and senescence-associated β-galactosidase activity. Notch-induced senescence involves canonical CSL/RBPJ-dependent transcriptional activity and the $p16^{INK4A}$-Rb pathway. Loss of $p16^{INK4A}$ or the presence of human papilloma virus (HPV) E6/E7 oncogene products not only prevented ICN1 from inducing senescence but permitted ICN1 to facilitate anchorage-independent colony formation and xenograft tumor growth with increased cell proliferation and reduced squamous-cell differentiation. Moreover, Notch1 appears to mediate replicative senescence as well as transforming growth factor-β-induced cellular senescence in non-transformed cells and that HPV E6/E7 targets Notch1 for inactivation to prevent senescence, revealing a tumor-suppressor attribute of endogenous Notch1. In aggregate, cellular senescence checkpoint functions may influence dichotomous Notch activities in the neoplastic context.

Oncogene advance online publication, 16 June 2014; doi:10.1038/onc.2014.169

INTRODUCTION

Esophageal squamous cell carcinoma (ESCC) is among the deadliest cancers known[1] and is a paradigm for the investigation of all types of squamous cell carcinomas (SCCs). Common genetic lesions associated with ESCC include p53 mutations, $p16^{INK4A}$ loss, cyclin D1 overexpression, epidermal growth factor receptor (EGFR) overexpression and telomerase activation.[2] Ectopically expressed telomerase (hTERT) or human papilloma virus (HPV) E6/E7 gene products immortalize human esophageal epithelial cells (keratinocytes) overcoming replicative senescence.[3,4] Oncogenes induce senescence in immortalized esophageal keratinocytes.[5–7] Senescence serves as a fail-safe mechanism to prevent oncogene-induced aberrant proliferation. In fact, malignant transformation of esophageal keratinocytes requires concurrent inactivation of the senescence checkpoint functions regulated by the p53 and Rb pathways to negate oncogene-induced senescence.[5,7–9]

The Notch pathway regulates cell fate and differentiation through cell–cell communication. The mammalian Notch family comprises four transmembrane receptor proteins (Notch1 to Notch4). Ligands (JAG1/2, DLL1, 3 and 4) bind Notch receptors through cell–cell contact to trigger γ-secretase-mediated proteolytic cleavage of Notch receptor proteins, resulting in nuclear translocation of the intracellular domain of Notch (ICN), the activated form of Notch. ICN of all Notch receptor paralogs forms a transcriptional activation complex containing a common transcription factor CSL (a.k.a. RBPJκ) and the coactivator Mastermind-like (MAML).[10] Notch1 target genes include the HES/HEY family of transcription factors, Notch3 and IVL, a marker of squamous-cell differentiation. Squamous-cell differentiation is impaired by *Notch1* loss, *CSL* loss or ectopic expression of dominant-negative MAML1 (DNMAML1) in the skin and esophagus in mice.[11–13]

The highly context-dependent nature of Notch functions adds complexity to its roles in cancers. Although Notch acts as an oncogene in T-cell acute lymphoblastic leukemia, both oncogenic and tumor-suppressor roles have been found in solid tumors even within identical tumor types.[14] Notch1 may be activated in SCCs.[15,16] The active form of Notch1 (that is, ICN1) transforms

[1]Gastroenterology Division, Department of Medicine, University of Pennsylvania, Philadelphia, PA, USA; [2]Abramson Cancer Center, University of Pennsylvania, Philadelphia, PA, USA; [3]Department of Gastroenterology and Hepatology, Hokkaido University, Sapporo, Japan; [4]Departments of Otorhinolaryngology–Head and Neck Surgery, University of Pennsylvania, Philadelphia, PA, USA; [5]Philadelphia VA Medical Center, Philadelphia, PA, USA; [6]Department of Pathology, Kochi University Medical School, Kochi, Japan; [7]Department of Therapeutic Oncology, Kyoto University Graduate School of Medicine, Kyoto, Japan; [8]Department of Gastroenterology and Hepatology, Okayama University Graduate School of Medicine, Dentistry, and Pharmaceutical Sciences, Okayama, Japan; [9]Department of Microbiology and Molecular Genetics, University of Pittsburgh School of Medicine, Pittsburgh, PA, USA; [10]Division of Biostatistics, Center for Clinical Epidemiology and Biostatistics, University of Pennsylvania, Philadelphia, PA, USA; [11]Department of Pathology, Fox Chase Cancer Center, Philadelphia, PA, USA; [12]Department of Medicine, Harvard Medical School, Boston, MA, USA; [13]Division of Cellular and Molecular Oncology, Dana-Farber Cancer Institute, Boston, MA, USA; [14]Department of Cancer Biology, University of Pennsylvania, Philadelphia, PA, USA and [15]Department of Genetics, University of Pennsylvania, Philadelphia, PA, USA. Correspondence: Dr H Nakagawa, Gastroenterology Division, Department of Medicine, University of Pennsylvania, 956 BRB, 421Curie Boulevard, Philadelphia, PA 19104-4863, USA.
E-mail: nakagawh@mail.med.upenn.edu
[16]These authors contributed equally to this work.
Received 7 October 2013; revised 27 March 2014; accepted 14 April 2014